# Transverse multibunch instability with a realistic 9-cell cavity in TESLA

A. Mosnier
Centre d'Etudes de Saclay, France

## 1 Introduction

We present some results on multibunch tranverse instability calculation applied to the proposed TESLA SC linear collider. The dipole modes of the 9-cell cavities and the expected Q for these modes were studied with Urmel calculations. Several schemes of constant beta FODO focusing were simulated for a given random displacement of the cavities with a rms value of 1 mm. We conclude that a rather weak focusing scheme (quadrupole spacing = 55 m) is sufficient to keep the emittance at the design value of $10^{-6}$ m rad. The effect of quadrupole position jitter is studied both anatically and with a tracking code. The tolerance in quadrupole alignment due to chromatic effect is not studied in this paper.

## 2 The 9-cell cavity

We consider the small iris aperture 9-cell cavity from ref. [2] scaled to 1300 MHz. Table 1 gives the 10 first highest coupling impedance non propagating dipole HOMs. The definition of the transverse impedance ( in $\Omega/m^2$ ) we use, is

$$R'/Q = \frac{1}{\omega W}\left|\int \nabla_\perp E_z\, e^{j k z}\, dz\right|^2 = \frac{2}{a^2}\, R/Q_{Urmel}$$

where a is the distance from the beam axis at which the field is integrated.
We assume the dipole modes are damped with a loop which couples to the axial magnetic field. The anticipated external Q's are estimated according the following formulae, which gives very good predictions for vanishing modes

$$Qex = \frac{\omega W}{P_{ex}} = \frac{2 R W}{\omega \mu^2 S^2 H_z}$$

The loop area is chosen equal to a moderate value S=1 $cm^2$ . We note that the obtained Q's are all below $10^5$ , except for one mode, without any coupling enhancement of the HOM coupler device.
Among the propagating modes, we have to worry about the trapped 5th passband, because these modes couple very poorly yo the beam tube. If one of the methods quoted in [2] is used to have the HOM couplers sitting near the peak of the standing wave pattern of these modes, we expect the resulting Q's of the table 2. We note that the modes which are not at all damped have fortunately very small R/Q.

| Mode | Frequency (MHz) | R'/Q ( $10^4$ ) | Qex ( $10^4$ ) | R'/Q * Qex ( $10^8$ ) |
|---|---|---|---|---|
| TM110 - 5π/9 | 1890.8 | 11.67 | 5 | 58.3 |
| TM110 - 4π/9 | 1898.1 | 3.75 | 8.4 | 31.5 |
| TM110 - 6π/9 | 1880.9 | 7.12 | 3.2 | 22.8 |
| TE111 - 7π/9 | 1764.2 | 13.63 | 0.55 | 7.5 |
| TM110 - 2π/9 | 1906.4 | 0.19 | 34.25 | 6.5 |
| TE111 - 6π/9 | 1741.2 | 11.35 | 0.5 | 5.7 |
| TM110 - 8π/9 | 1852.0 | 1.26 | 1.4 | 1.8 |
| TE111 - 8π/9 | 1788.0 | 1.45 | 0.6 | 0.9 |
| TE111 - π | 1811.2 | 1.0 | 0.75 | 0.7 |
| TE111 - 4π/9 | 1701.7 | 0.73 | 0.6 | 0.4 |

Table 1 : R/Q and calculated Qex of the 10 first highest coupling impedance non propagating modes

| Frequency (MHz) | R'/Q ( $10^4$ ) | Qex | R'/Q * Qex ( $10^8$ ) |
|---|---|---|---|
| 3081.6 | 0.0006 | $10^9$ | 60 |
| 3082.4 | 0.0044 | $10^9$ | 440 |
| 3084.1 | 0.0017 | $10^9$ | 170 |
| 3087.0 | 0.2100 | $5\ 10^6$ | 105 |
| 3091.8 | 1.2000 | $10^6$ | 120 |
| 3099.9 | 1.2000 | $10^5$ | 12 |

Table 2 : R/Q and predicted Qex of the trapped 5th passband

## 3 The machine parameters

We consider the two machines "Top-Factory" and "1/2 Tesla" defined in [3]. The useful parameters for Beam Break Up calculations are listed in table 3.

| Parameters | Top-Factory | 1/2 Tesla |
|---|---|---|
| Energy (GeV) | 125 | 250 |
| Injection energy (GeV) | 3 | 3 |
| Number of bunches | 800 | 800 |
| Bunch separation (μS) | 0.4 | 1.0 |
| Peak current (mA) | 8 | 8.224 |
| Eacc (MV/m) | 12.5 | 25 |
| Total number of cavities | 10000 | 10000 |

Table 3 : List of the parameters for the two machines considered.

The focusing scheme is a FODO lattice with constant phase advance and beta function all along the linac.

## 4 The multibunch transverse stability

Following the idea in [4] , we study the multibunch instability generated by cavity misalignments rather than by offsets of the injected bunches. The train of 800 bunches is tracked through the 10000 cavities and the emittance growth is computed at the end of the linac. We have to check that the resulting emittance growth due to cumulative BBU is much smaller than the horizontal normalized emittance design value of $10^{-6}$ m rad.

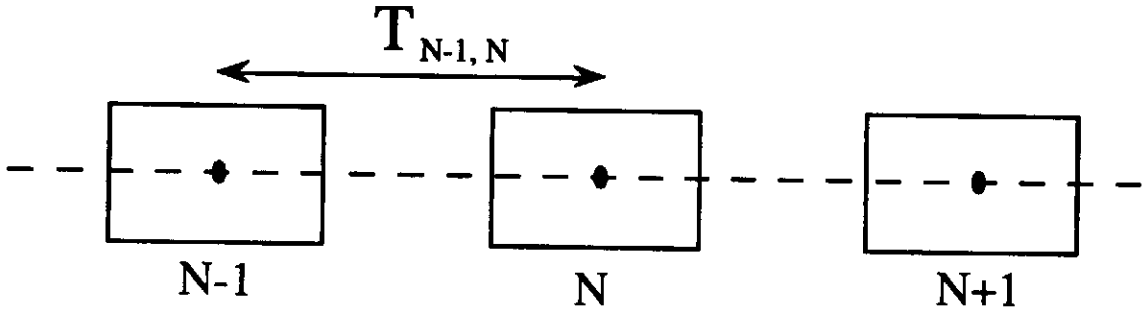


The coordinates of the bunch k at the entrance of the cavity N is given in terms of its coordinates at the entrance of the cavity N-1.

$$\begin{bmatrix} x_{N(k)} \\ x'_{N(k)} \end{bmatrix} = T_{N-1,N} \begin{bmatrix} x_{N-1(k)} \\ x'_{N-1(k)} \end{bmatrix} + \begin{bmatrix} 0 \\ \Delta p_{\perp} / p_{z\,N} \end{bmatrix}$$

where $T_{N-1,N}$ is the transport matrix from the center of the cavity N-1 to the center of the cavity N and includes the adiabatic damping due to the acceleration. The kick given by the cavity N-1 is the result of the wakefields induced by all the preceding bunches

$$\Delta p_{\perp} = \frac{e\,Q_b}{2} R'_{\perp}/Q \sum_{L=1}^{M-1} s_{M-L}\, x_{N-1}(L)$$

$$\text{with} \quad s_K = e^{-k\,\omega_r \tau / 2Q} \sin k\,\omega_r \tau$$

When many HOM's are studied, the induced fields must be added up.
The cavity alignment errors are randomly generated with a gaussian distribution. The standard deviation is fixed to $\sigma_{offset} = 1$ mm with a distribution truncated at $\pm 2\,\sigma$. In the same way, as the mode frequency varies from cavity to cavity due to fabrication tolerances, each mode has a frequency dispersion of $\sigma_{freq} = 1$ MHz. We note that the frequency spread of 1 MHz is far above the mode bandwidths ( about 50 times for a Q of $10^5$ ) and is large enough to cancel any resonant buildup of the fields. We find that larger frequency spreads have no significant effect on the resulting emittance growth. For example, figure 1 is the histogram of the frequencies for one mode during a simulation with 10000 cavities. The CPU time used for one simulation is about 150 seconds on a CRAY computer.

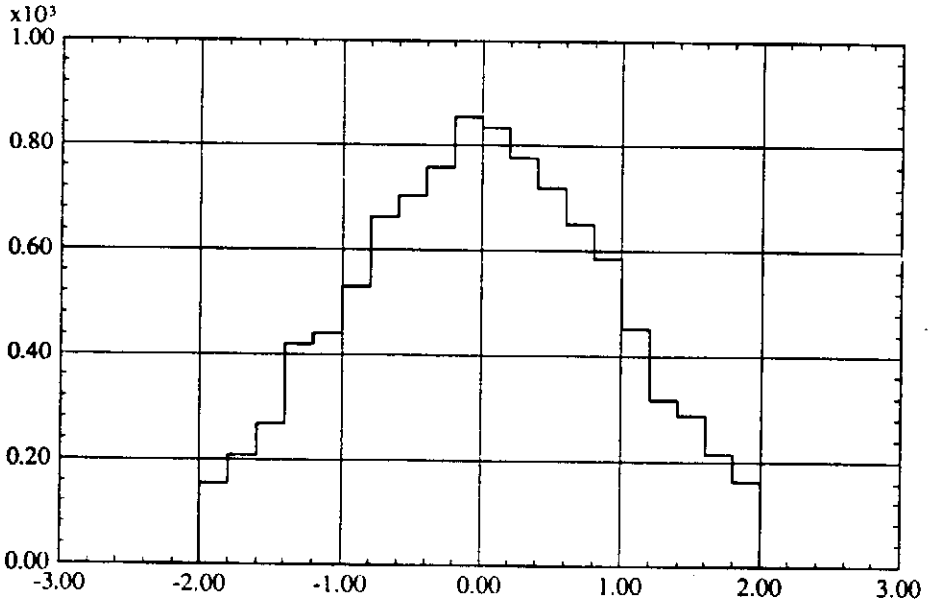


Figure 1 : Example of histogram of the frequencies for one mode during a simulation

# 5 Results of BBU simulations with non propagating HOM's

Since a decrease of the bunch spacing is equivalent to an increase of the Q of the modes and the bunch perturbation is higher for a less accelerating linac, the multibunch instability will be hence stronger in the 125 GeV machine than in the 250 GeV machine. The simulations are performed first on the "Top-Factory" and we have checked that, for the same focalisation scenario, the emittance dilution is smaller in the higher energy machine (2 to 3 times lower). Figure 2 shows for example the tranverse displacements of the 800 bunches at the exit of the 10000-cavity linac with 10 HOMs and the phase space coordinates, from which the emittance growth is computed, is given on figure 3

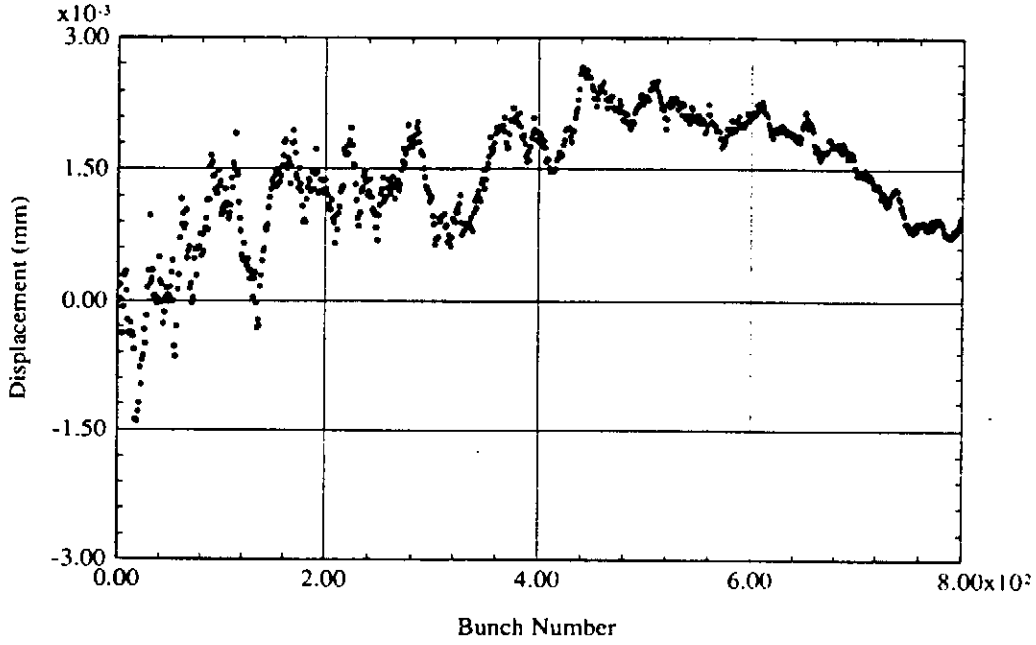


Figure 2 : Transverse displacement of the 800 bunches emerging from the linac

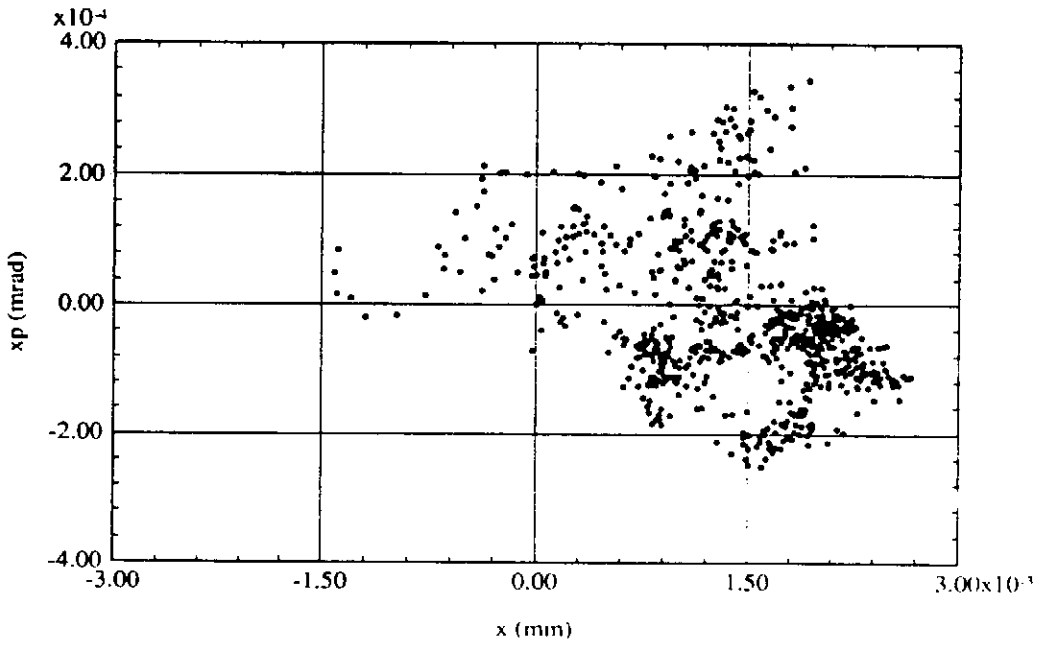


Figure 3 : Phase space coordinates of the 800 bunches emerging from the linac.

We study now the multibunch instability driven by the ten non propagating modes listed in table 1. We know that more the FODO cell will be long and more the tolerances on the quadrupole offsets will be relaxed. But what is the maximum cell length permissible from the point of view of the cumulative BBU ? We compute therefore the dependance of the emittance growth on the FODO lattice - length and phase advance - and on the Q of the modes.

## 5.a The FODO cell length dependance

Since we find that the seed of the random generator, particularly for cavity position, has a significant effect on the blow up, the simulations are repeated several times with different seeds for each set of parameters. Figure 4 gives the normalized emittances for different seeds when the number of cavities between two adjacent quadrupoles is varied. The phase advance per cell was set to 90°. A module of 8 cavities is about 11 m long. The result is that the emittance growth vary approximatively linearly with the FODO cell length. We conclude that, if the Q's of table 1 can be obtained, a constant beta FODO lattice with one quadrupole every 40th cavity is sufficient to guarantee an emittance dilution much smaller than the design value.

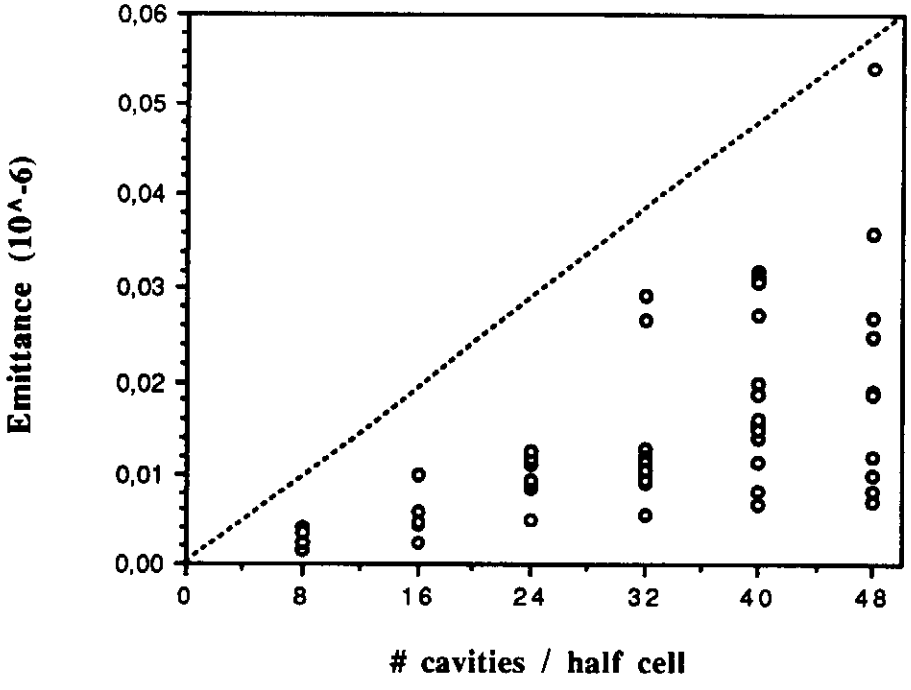


Figure 4 : Emittance growth with different number of cavities per half FODO cell for $\mu = 90°$.

## 5.b The lattice phase advance dependance

The number of cavities per half cell and the total number of quadrupoles are now set to respectively 40 and 250. Figure 5 shows the effect of the phase advance. As before the blow up was computed for different seeds at each phase advance point. The emittance growth decreases as expected when the phase advance increase.

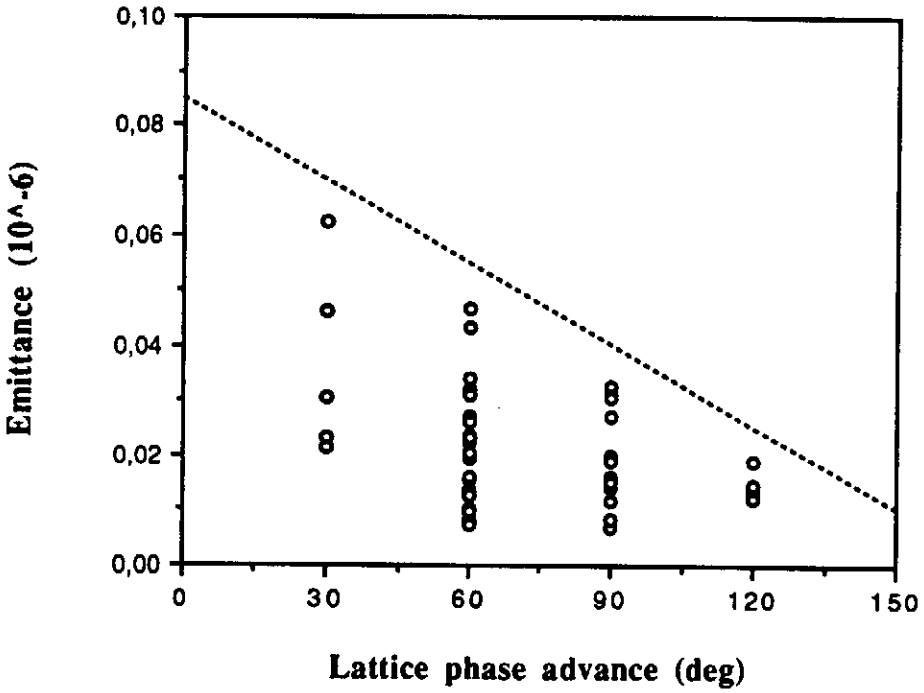


Figure 5 : Emittance growth with different FODO phase advances for one quadrupole every 40th cavity.

## 5.c HOM external Q dependance

The number of cavities per half cell and the total number of quadrupoles are again set to respectively 40 and 250 and the same seed is used when the Qs are varied. The Qs of all the 10 modes are varied by the same factor. Figure 6 shows the increase of emittance with the Q. The Q value in abscissa is the Q of the first HOM of the table 1. We see that, as long as the Q of the first mode is lower than $10^5$, the emittance dilution is tolerable.

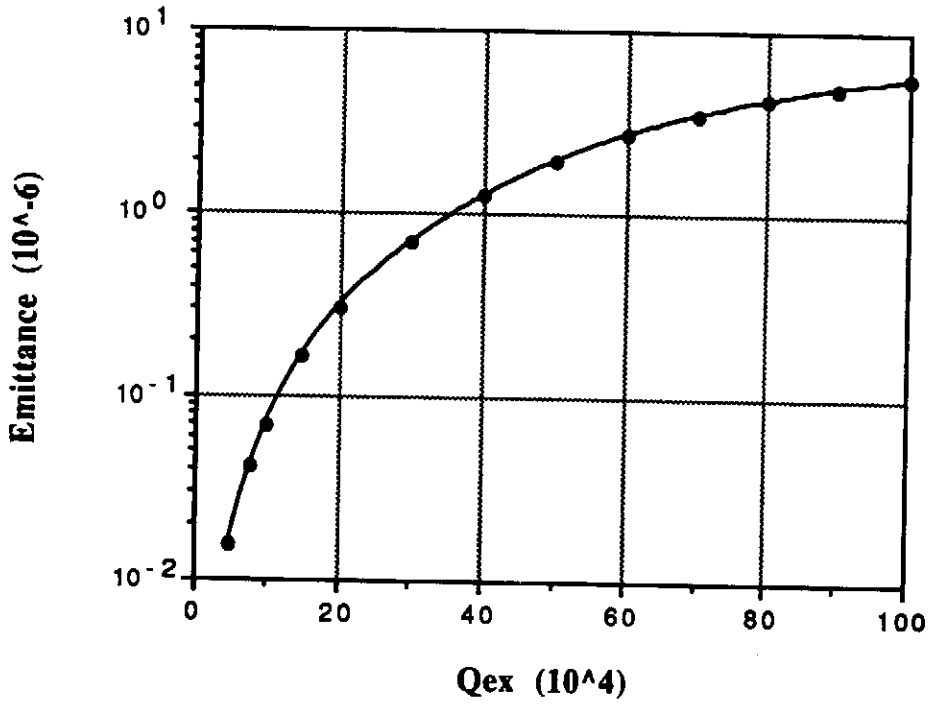


Figure 6 : Emittance growth with different Qex.

# 6 Results including the trapped HOM's

We study now the multibunch transverse instability driven by the trapped modes of the 5th dipole passband quoted in table 2, where we assumed that care was taken to have the HOM coupler sitting near the peak of the field standing wave pattern for the highest R/Q modes. We find that the bunch perturbation induced by only these trapped modes is of the same order of magnitude than the perturbation induced by the 2 first non propagating passbands. Figure 7 shows the bunch displacement at the exit of the 125 GeV linac caused by only these trapped modes with the following set of parameters :

| | |
|---|---|
| Number of cavities per half FODO cell | 40 |
| Total number of quadrupoles | 250 |
| Phase advance per FODO cell | 90° |

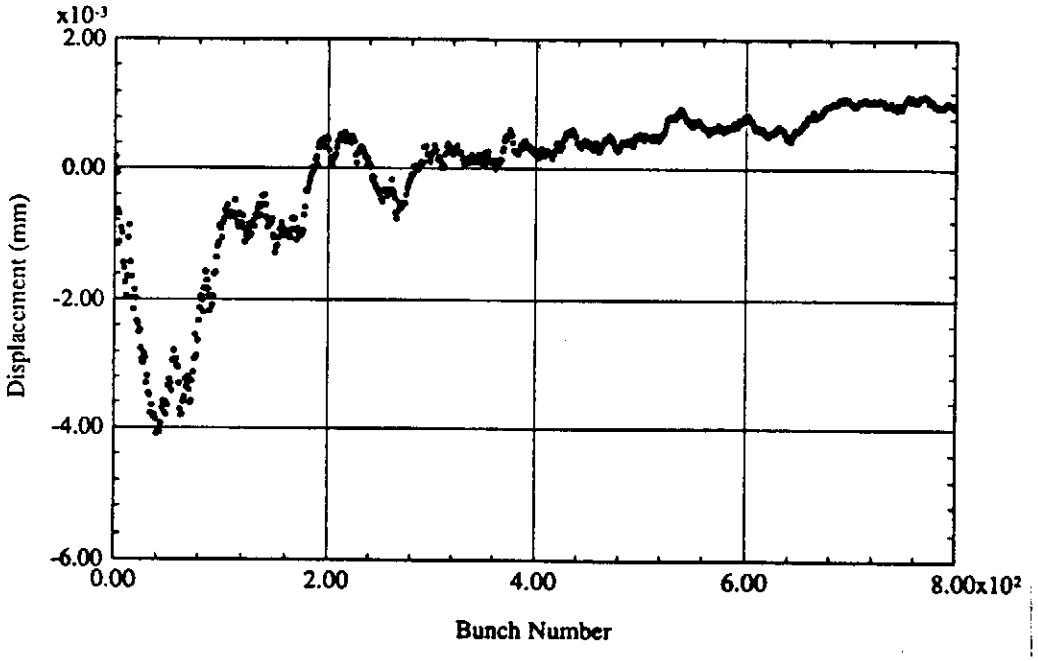


Figure 7 : Transverse displacement of the 800 bunches emerging from the linac

If we now include the effects of the ten first non propagating modes plus the six trapped modes, we obtain a maximum emittance growth of 0.07 $10^{-6}$, among the tested seeds, about 2 times higher than the emittance growth caused by only the 10 vanishing modes. When the Q of these trapped modes is increased, the effect of these modes dominates. For example, a Q enhancement factor of 5 with respect of table 2 leads to an emittance growth of about 0.15 $10^{-6}$. We conclude that we have to pay special attention to the damping of the 5th passband modes in the design of the cavity.

# 7 Tolerance on quadrupole position jitter

The beam displacement at the exit of the linac is the summation of all the betatron oscillations excited by the misaligned quadrupole kicks [1].

$$x_{ex} = \sum_i \frac{\beta_0}{f_0} d_i \left(\frac{\gamma_i}{\gamma_{ex}}\right)^{1/2} \sin(\psi_{ex} - \psi_i)$$

A constant focalisation scheme has been assumed (focal length $f_0$ and beta function $\beta_0$). $\Psi$ is the phase advance of the lattice and $d_i$ is the quadrupole position error. The adiabatic damping of the oscillations, due to the acceleration, has been included. The quadratic average of random uncorrelated quadrupole errors is

$$\langle x_{ex}^2 \rangle = \sum_i \left(\frac{\beta_0}{f_0}\right)^2 \langle d^2 \rangle \left(\frac{\gamma_i}{\gamma_{ex}}\right) \sin^2(\psi_{ex} - \psi_i)$$

For a large number of quadrupoles, we can replace the sum by an integral

$$x_{rms} = \left(\frac{\beta_0}{f_0}\right) d_{rms} \frac{\sqrt{N}}{2}$$

where N is the total number of quadrupoles. The resulting normalized emittance is then given by

$$\varepsilon_N = 4 \gamma_{ex} \frac{x_{rms}^2}{\beta_0} = \gamma_{ex} \frac{\beta_0}{f_0^2} N d_{rms}^2$$

in term of the phase advance $\mu$ and the FODO half cell length L, this can be written

$$\varepsilon_N = 4 \gamma_{ex} \tan \mu/2 \frac{N}{L} d_{rms}^2 \qquad (1)$$

We note that the number of quadrupoles being inversely proportional to the lattice length L, the emittance scales like $L^{-2}$.
Figure 8 shows the emittance versus the half cell length from equation (1) for a standard deviation of misalignment $d_{rms} = 0.1$ µm and a phase advance per cell $\mu = 90°$ in the 125 GeV linac. The circles are the results of simulations of bunches meeting randomly misaligned quadrupoles along a 125 GeV machine with 10000 cavities. For this motion magnitude, only half cell length above 20 m leads to emittance growth smaller than the horizontal emittance design value of $10^{-6}$. In the case studied above of 40 cavities between quadrupoles (L ≈ 55 m) a jitter of a few tenth of µm could be tolerated.

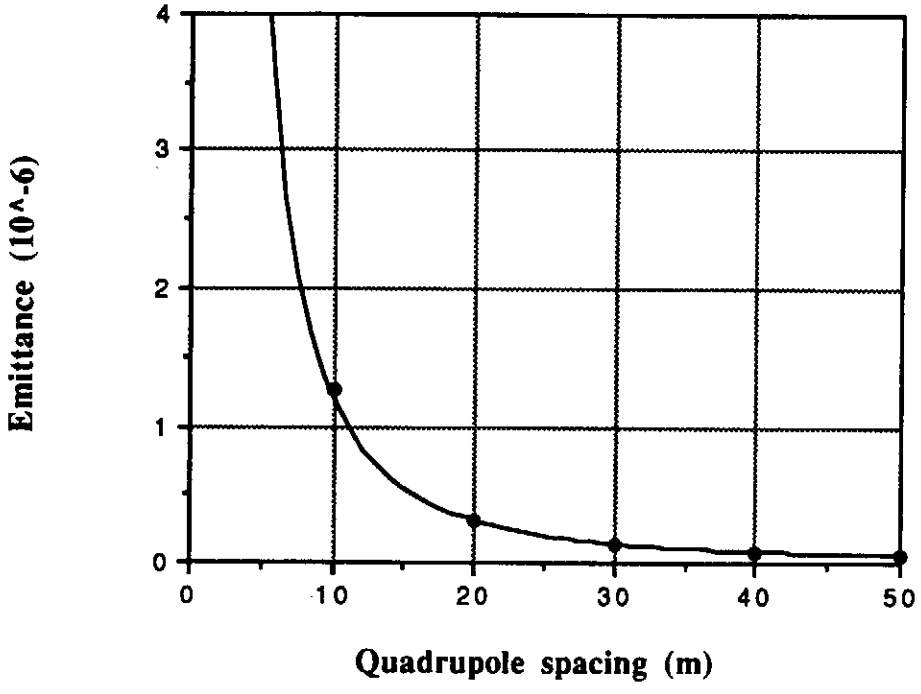


Figure 8 : Emittance versus the half cell length
for a rms quadrupole jitter of 0.1 μm

## References

[1] R.D. Ruth, SLAC-PUB-4436 (1987)
[2] E. Haebel and A. Mosnier, "Large or small iris aperture in SC multicell cavities ?" to be published in the proceedings of the 5th SRF Workshop (DESY, August 91)
[3] 5th SRF Workshop, TESLA session (DESY, August 91)
[4] G.A. Krafft et al., "Emittance growth in TESLA", Proceeding of the 1991 Part. Acc. Conf., San Francisco